Water Practice & Technology

 Water Practice & Technology Vol 19 No 3, 646 doi: 10.2166/wpt.2024.041

Estimating the percentage effects of Bemacid red dye adsorption dynamic parameters using a full factorial design approach

Fouzia Ouazani*, Sofiane Guella, Yassine Khalfi and Khedidja Benouis
Laboratory of Process Engineering, Materials and Environment, Faculty of Technology, University of Djillali Liabes, P.O. Box 89, Sidi Bel Abbes 22000, Algeria
*Corresponding author. E-mail: fouzia.ouazani@univ-sba.dz

ABSTRACT

In this study, we investigate the removal of Bemacid red dye using brewery waste in a packed bed column. We examined the effects of bed height, inlet flow, and inlet dye concentration on the column dynamics of adsorption. To assess the favorable column dynamics, we analyzed the breakthrough curves (BTCs). We also used the Clark, Thomas, Bed Depth Service Time (BDST), and Adams-Bohart models to determine the kinetic constants of the adsorption column from the obtained results of the dynamic studies curve of the BTCs. Analysis of the BTC studies revealed that both the BTCs time and worn-out time values increased with an increase in bed height and inlet Bemacid red dye dosage but decreased with an increase in the inlet flow rate. The results further showed that Thomas' model was the most suitable for describing the entire BTCs ($R^2 > 0.93$). Using a full factorial design to estimate the percentage effects of cited dynamic parameters, we found that these parameters accounted for 98% of the adsorption capacity. This methodology for estimation provides crucial information on the effects of parameters and the extent to which the adsorption capacity depends on the studied parameters.

Key words: adsorption, design expert, dynamics models, full factorial design, low-cost biosorbent, packed bed column

HIGHLIGHTS

- Brewery wastes are an efficient adsorbent for the removal of Bemacid red dye.
- The increase in the bed height of the column enhances the efficiency of the adsorption column.
- An increase in the initial dye concentration and flow rate weakens the efficiency of the adsorption column.
- Operational factors have an 89% dependency rate on the adsorption capacity.
- The experimental data are in agreement with the estimated data obtained through the full factorial design.

GRAPHICAL ABSTRACT

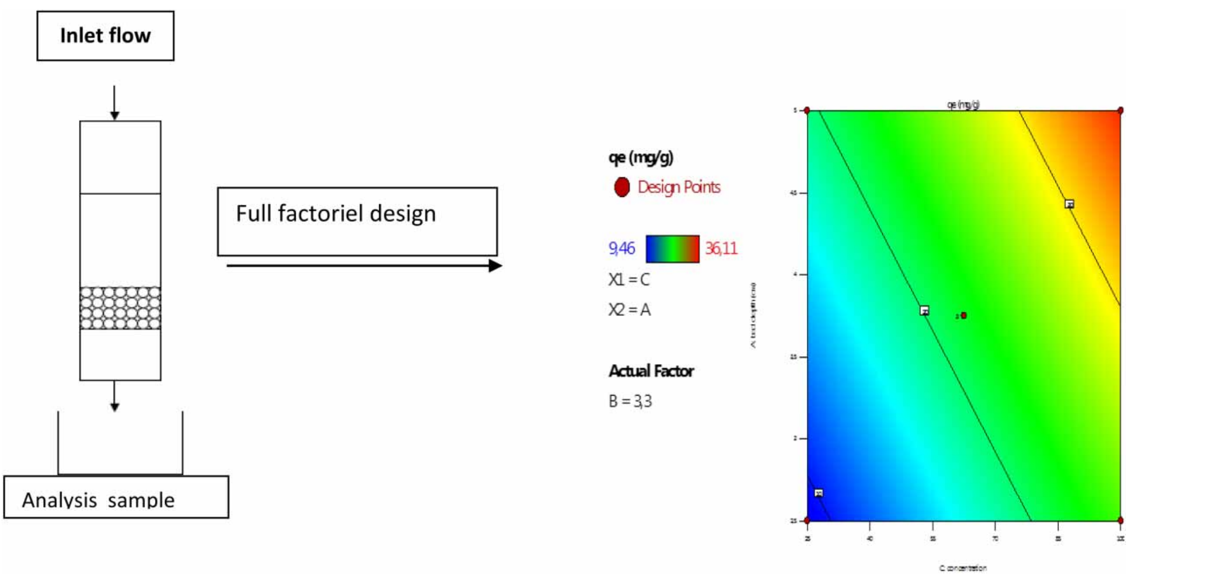

INTRODUCTION

Textile industries have used increasingly large quantities of industrial dyes, leading to a corresponding increase in the quantity of unloaded wastewater. The presence of these dyes in wastewater gives it an unattractive color and has negative effects on aquatic ecosystems, including the reduction of the permeation of light and photosynthesis (Zümriye 2005; Yagub *et al.* 2014).

To address the issue of water pollution, various treatment processes have been utilized to remove dyes from wastewater. These methods include oxidation, coagulation and flocculation, biological treatment, membrane filtration, and others. Of these, the adsorption process has emerged as the simplest and most effective alternative treatment for removing dyes from wastewater (Wong *et al.* 2004; Crini & Badot 2008; Almeida & Corso 2014). Activated charcoal is the most commonly used adsorbent in the adsorption process, but its relatively high cost often limits its usage (Gupta & Suhas 2009; Mobasherpour *et al.* 2014). As an alternative, it is recommended to utilize low-cost adsorbents, such as industrial waste materials like those from the steel and fertilizer industries (Jain *et al.* 2003), brewery waste (Ouazani *et al.* 2017), natural materials (Bulgariu *et al.* 2019), or agricultural by-products (Bharathi & Ramesh 2013). The adsorption technique can be performed using either batch or continuous modes (Bharathi & Ramesh 2013). The batch mode is typically used in laboratory-scale experiments but is not suitable for industrial applications due to the continuous flow of pollutants and the large volumes involved. In contrast, the continuous mode (or dynamic mode) is suitable for large-scale applications in wastewater treatment due to its flexibility and ease of operation (García-Mateos *et al.* 2015).

The breakthrough curve (BTC) obtained from the dynamic study provides significant insights into the dynamic behavior of the adsorption column and is crucial for designing, optimizing, and operating the separation process. Several dynamic models, such as the Bed Depth Service Time (BDST) model, Clark model, Yoon-Landon model, Adams-Bohart model, and Thomas model, are utilized to evaluate and predict the efficiency of the column (Kyzas *et al.* 2012; Sicupira *et al.* 2015; Yang *et al.* 2015).

In this study, the feasibility of using brewery waste as a low-cost adsorbent for the removal of ETL dye in a packed bed column adsorption process was investigated. The effects of various dynamic factors such as bed height, inlet ETL dye concentration, and flow rate were evaluated in a continuous column adsorption system. The kinetic constants of the BTCs were determined and optimized using the different dynamic models. The percentage of dependence between dynamic factors and adsorption capacity is estimated by using the full factorial design.

MATERIALS AND USED TECHNIQUES

Adsorbent and adsorbate

In our previous study (Ouazani *et al.* 2017), we described of brewery waste. Based on the results of Fourier Transform Infra Red (FTIR) analysis, it was found that the waste contains lignin and cellulose, classifying it as a lignocellulosic adsorbent. The ETL dye, which is used in this study, is an industrial dye commonly used in the textile industry. The dye was obtained from the SOITEX plant in Tlemcen, which is located in western Algeria. The structure of the dye is unknown, and the solution used in this study was prepared by dissolving 1 g of the ETL dye in 1 L of distilled water.

The spectrophotometer analysis UV-Visible (HACH DR 2000) is utilized to measure the residual concentration of samples at 500 nm.

Fixed-bed column study

The study on fixed-bed column adsorption involved packing a specific amount of brewery waste into a glass column with an internal diameter of 1.1 cm and a length of 20 cm. The column was then subjected to a controlled flow rate of ETL dye solution at a predetermined concentration. At predetermined time intervals, samples were collected and analyzed to determine the remaining concentration of ETL dye. The impact of various operational parameters, including bed height (2.5–5 cm), feed flow rate (1.5–5.1 mL/min), and inlet ETL dye concentration (25–100 mg/L), was investigated. The effectiveness of the packed bed was determined by analyzing the BTC, which plots the concentration of adsorbed dye against time. The efficiency of the packed bed can also be represented by the normalized concentration, which is the ratio of the residual dye concentration to the inlet dye concentration (C/C_0), plotted against either flow time (t) or effluent volume ($V_{eff} = Q^* t_{total}$). From this formula, the t_{total} and Q are the total process time (min) and volumetric flow rate (mL/min), respectively (Kannan *et al.* 2012; Pei-Jen *et al.* 2014).

To assess the experimental results and make the packed bed suitable for industrial applications, various models such as Adams-Bohart, Thomas, Clark, and BDST were employed to analyze the performance of the packed bed.

Thomas model

The Thomas model is used to describe the jamming behavior of flow in the fixed bed, employing the Langmuir isotherm and the parameters of the second-order kinetic model. This model is particularly useful for adsorption processes where the effects of external and internal diffusion are negligible (Hutchins 1973), and the equation of this model is (Ming-Shen & Hsing-Ya 2002; Muhamad *et al.* 2010; Gassan *et al.* 2014) as follows:

$$\mathrm{Ln}\left(\frac{C_0}{C}-1\right)=\frac{K_T q_0 M}{Q}-K_T C_0 t \tag{1}$$

Equation (1) can be used to determine the rate constant (K_T) and the adsorption capacity (q_0) of the packaged bed. M is the weight of the adsorbent (g), Q is the flow (L/min), and C is the residual concentration of the Adsorbat in time t. The K_T and q_0 coefficients can be calculated by plotting Ln ($C_0/C-1$) against time (t) (Hameed 2009).

The Adams-Bohart model

The Adams-Bohart model assumes that the amount of adsorption is dependent on both the adsorbent and the residual effluent dosage and is expressed as follows (Nkem *et al.* 2011):

$$\mathrm{Ln}\left(\frac{C_0}{C}-1\right)=K_{AB}N_0\frac{Z}{V}-K_{AB}C_0 t \tag{2}$$

where K_{AB} is the Adams-Bohart constant rate (L/mg·min), V is the cumulative liquid throughput volume (cm/min) and N_0 the adsorption amount per volume unit (mg/L).

Clark model

The model utilized the Freundlich isotherm in conjunction with the concept of mass diffusion (Ghosh *et al.*, 2015). The equation for the model (Equation (3)) includes the Clark constants A and r, as well as the Freundlich parameter n.

$$\left(\frac{C}{C_0}\right)^{n-1}-1=Ae^{-rt} \tag{3}$$

The BDST model

The BDST model is commonly used to establish a relationship between the bed height (Z), service time (t), and adsorption parameters (Sekhula *et al.* 2012). The equation for the BDST model is given by the following equation:

$$\mathrm{Ln}\left(\frac{C_0}{C}-1\right)=\mathrm{Ln}\left(e^{K_{AB}N_0\frac{Z}{V}}-1\right)-K_{AB}C_0 t \tag{4}$$

Hutchins (1973) proposed an equation to establish a linear relationship between bed height and service time, as shown in Equation (5):

$$t=\frac{N_0 Z}{C_0 V}-\frac{1}{K_{AB}C_0}\,\mathrm{Ln}\left(\frac{C_0}{C}-1\right) \tag{5}$$

The quantity of dye captured by the fixed bed is denoted by the area under the BTC (C versus t) and can be determined through numerical integration (Sicupira *et al.* 2015). The ratio of the dye mass (m_{ad}) and the adsorbent mass (M) can be used to determine the capacity (q) of the packed bed.

RESULTS AND DISCUSSION

The performance of the continuous fixed-bed column process was depicted by plotting the BTC, which shows the relationship between the residual dye concentration and the dye inlet concentration (C_{res}/C_0) as a function of operating time (t).

Influence of bed depth on column efficiency

Figure 1 shows the BTCs of ETL dye adsorption obtained under the following operational conditions: bed depths of 25, 35, and 50 mm, a flow rate of 1.5 mL/min, and an inlet dye dosage of 25 mg/L. It can be observed that increasing the bed depth resulted in a longer contact time for adsorption within the column. The increase in bed depth resulted in a larger service zone available for adsorption and an increase in the number of active adsorbent sites (Zümriye & Gönen 2004). Consequently, the breakthrough time and the exhaustion time increased from 6 to 84 and 17 to 542 min, respectively, when the bed depth was increased from 25 to 50 mm. The most effective bed depth in the adsorption column was 50 mm, corresponding to 1.42 g of brewery waste, as it resulted in the slowest breakthrough among the tested bed depths (Figure 1). As the bed depth decreased, the breakthrough of the dye occurred more rapidly and the packed bed column was depleted more quickly, leading to decreased efficiency. The bed depth had a significant impact on both the breakthrough time and bed efficiency of the column. Similar observations were made for other flow rates and concentrations. The findings of this study were consistent with those of previous studies on the adsorption of methylene blue and diazo dye Brilliant Black BN by chitosan beads, as reported by Chowdhury *et al.* (2016) and Shadeera & Nagapadma (2015), respectively.

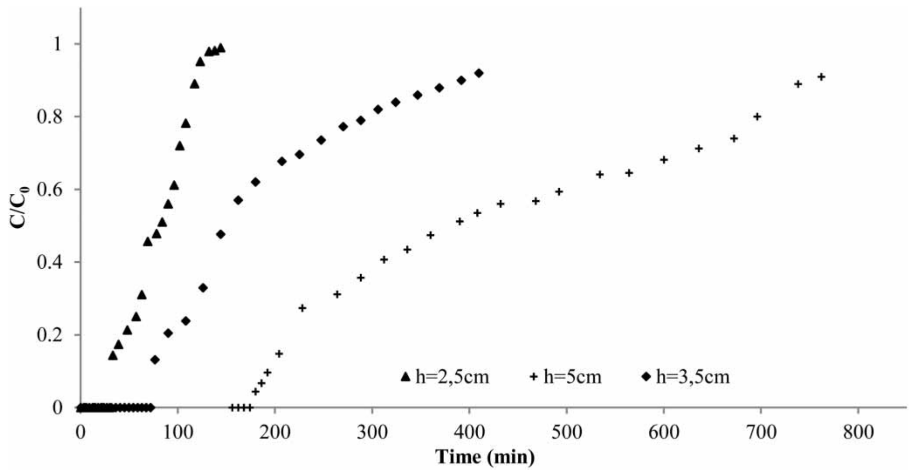

Figure 1 | Influence of bed depth on ETL dye column efficiency.

Influence of the flow rate on ETL dye column efficiency

Various factors affect the adsorption capacity of a fixed-bed column, including the inlet dye flow rate. In this research, the flow rates ranged from 1.5 to 5. 1 mL/min, while the bed depth and dye concentration remained constant. Figure 2 shows that the BTCs for the dye adsorption process decreased as the inlet dye flow rate increased from 1.5 to 5.1 mL/min. This indicates a shorter operational column time. This suggests that a higher dye flow rate leads to a shorter operating time for the column. This can be explained by the fact that at a fast inlet flow rate, the dye molecules do not have enough time to reach adsorption equilibrium and exit the column before equilibrium is achieved. However, at a lower inlet flow rate, the residence time of the dye molecules in the column is increased, allowing for sufficient contact time with the adsorbent. Thus, a lower flow rate results in a higher removal of dye molecules in the column. These findings are consistent with those reported by Al-Baidhany & Al-Salihy (2016).

Influence of initial dye concentration on ETL dye column efficiency

Figure 3 shows the BTCs obtained for ETL dye adsorption at concentrations of 25 and 100 mg/L, with the fixed inlet flow rate (1.5 mL/min) and bed depth (5 cm). At the lower dye concentration, a longer time was needed for the active sites of the brewery waste to be saturated due to the lower amount of adsorbate and slower transport of

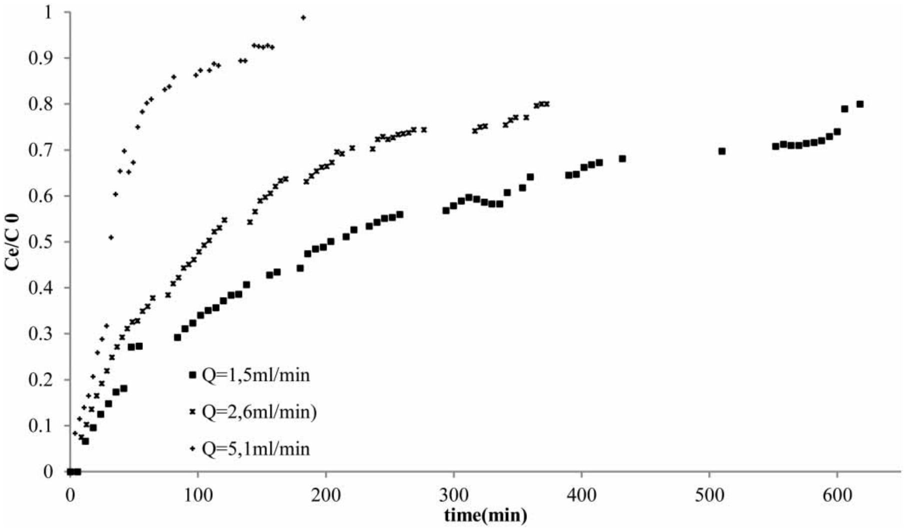

Figure 2 | Influence of flow rate on ETL dye column efficiency.

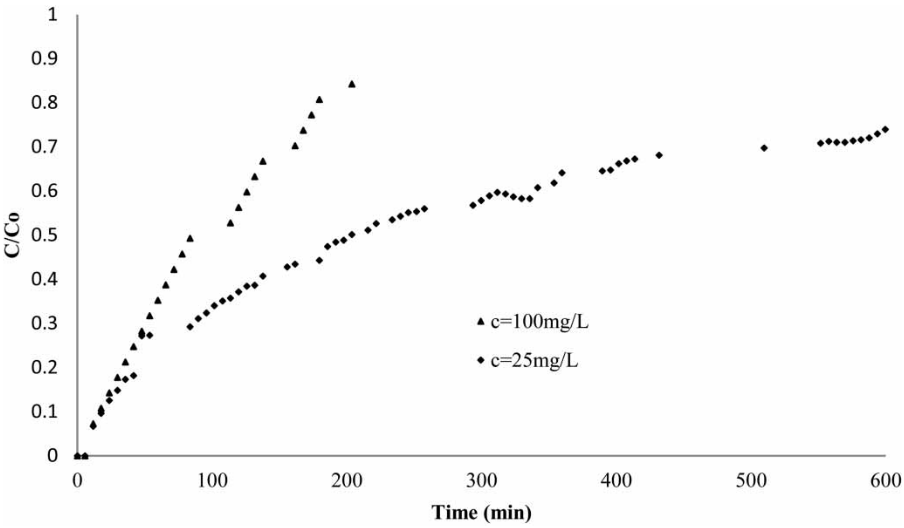

Figure 3 | Influence of initial dye concentration on ETL dye column efficiency.

dye molecules (Nishil *et al.* 2015). This finding is consistent with previous studies (Nouri & Ouederni 2013; Nihla *et al.* 2015). However, the adsorption capacity increased from 6.44 to 73 mg/g when the inlet ETL dye dosage was raised from 25 to 100 mg/L.

Assessment of breakthrough curves and determination of kinetic parameters

In our study, we used the column service time when the normalized concentration (C/C_0) reaches 0.05 based on the data of previous research (Mobasherpour *et al.* 2014; Nishil *et al.* 2015). The relationship between the bed altitude (Z) and time (t) at a flow rate of 1.5 mL/min is plotted in Figure 4, which represents a linear relationship described by Equation (4) with a determination coefficient (R^2) above 0.98. This indicates that the BDST model is suitable for the studied column system. Using the BDST model, the estimated values for the adsorption capacity (N_0) and rate constant (K_{AB}) are 14.1 mg/L and 3.64 cm^3/mg·min, respectively. The advantage of the BDST model is that it allows for the reliable scaling of experimental data to other inlet flow values without further experimentation (Nouri & Ouederni 2013).

The bed data were fitted with three different dynamic models previously cited to determine the rate constant (K_{AB}) and maximum adsorption capacity (q). The results for the two kinetic parameters (K_{AB}) and (q) and their determination coefficients are presented in Table 1. The obtained results indicate that the Clark model provided a

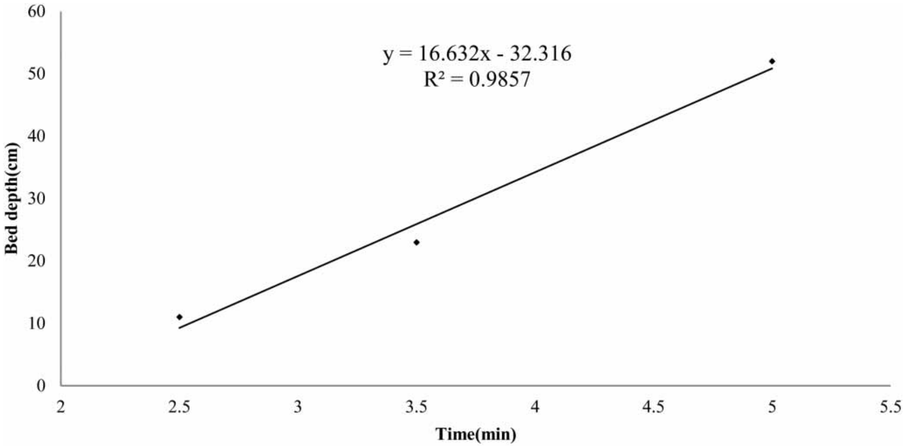

Figure 4 | BDST model of ETL dye-packed bed column breakthrough.

good fit to the experimental data, with determination coefficients ranging from 0.94 to 0.97 for all operational conditions. Furthermore, Table 1 reveals that the value of the kinetic constant was influenced by the flow rate, inlet dye concentration, and bed depth. It was observed that the bed capacity (q_0) was inversely proportional to the flow rate but proportional to the inlet dye concentration.

According to the results presented in Table 1, the values of the kinetic constants obtained using the Adams-Bohart model remained constant for the operational conditions where the dye concentration was 25 mg/L and the flow rate was 1.5 mL/min, regardless of the bed altitude. However, for other conditions, a slight variation in the K_{AB} constant was observed. These findings suggest that the bed depth did not have a significant impact on the values of the kinetic constant.

The estimated values of the kinetic constant K_{AB} in this study were found to be lower than the values reported by Hamdaoui (2006) for the removal of methylene blue using sawdust of cedar, which was 34×10^{-3} L/mg·min at an altitude of 8 cm and a flow rate of 23 mL/h. On the contrary, the volume capacity obtained in this study is higher than the value reported by Bennani *et al.* (2015) when they used Moroccan clay for the removal of basic red dye 46, which was 160 mg/L under the operational conditions of a dye concentration of 160 mg/L, a bed depth of 15 cm, and a flow rate of 4 mL/min.

The results presented in Table 1 indicate that the Thomas rate constant K_T values vary significantly under different operational conditions. For instance, when the inlet dye concentration is 25 mg/L and the flow rate is 1.5 mL/min, the K_T value ranges from 2×10^{-3} to 22.4×10^{-3} L/mg·min, and a similar trend is observed for other flow rates.

The estimated values of the Thomas rate constant K_T in this study are higher than those reported in previous research. For instance, Sivakumar & Palanisamy (2009) found a rate constant of 1.4 mL/mg·min for the removal of acid blue dye 92 using activated charcoal at an initial concentration of 25 mg/L and a bed height of 5 cm. Similarly, Shadeera & Nagapadma (2015) reported a rate constant of 0.35 mL/mg·min for the removal of Brilliant diazo dye at a concentration of 20 mg/L, a bed height of 6 cm, and a flow rate of 0.8 m/min. However, the values obtained in this study are within the same range as those reported by Manase (2012) for the removal of Rhodamine B using activated charcoal.

Table 1 shows that the Clark constant r ranges from 0.11 to 0.73 min^{-1}. These values are higher than those obtained for the removal of methylene blue dye (ranging from 0.02 to 0.07 min^{-1}) as reported by Hamdaoui (2006). Notably, the highest value of the Clark constant r (0.73 min^{-1}) was observed for a bed altitude of $h =$ 2.5 cm, a flow rate of 1.5 mL·min^{-1}, and an initial dye concentration of 100 mg/L. Furthermore, the variation in the Clark constant r was insignificant when the altitude was increased from 2.5 to 5 cm, suggesting that altitude has no influence on the constant for a consistent flow rate.

Full factorial design for optimizing the effects of operational parameters

In our adsorption column study, it was found that the adsorption process of ETL dye on brewery waste was affected by inlet ETL dye dosage, bed altitude, and flow rate. A statistical study was conducted to optimize these factors and model the adsorption capacity in the experimental area.

Table 1 | Kinetic parameters of ETL dye packed bed column

ETL dye concentration	25 (mg/l)									100 (mg/l)								
Bed depth	2.5 (cm)			3.5 (cm)			5 (cm)			2.5 (cm)			3.5 (cm)			5 (cm)		
Flow rate (mL/min)	1.5	2.6	5.1	1.5	2.6	5.1	1.5	2.6	5.1	1.5	2.6	5.1	1.5	2.6	5.1	1.5	2.6	5.1
Thomas model																		
K_T (L/mg·min) $\times 10^3$)	22.4	10	15.6	4.4	7.6	4.4	2	20	11.2	1.4	4.9	3.5	1.7	3	2.9	1.4	2.5	2.1
q_0 (mg/g)	2.86	4.19	7.42	5.83	5.87	5.83	10.47	10.4	8.77	3.69	13.2	7.2	13.2	18.3	18.7	12.2	16.6	31.7
R^2	0.94	0.95	0.97	0.93	0.97	0.93	0.94	0.92	0.92	0.96	0.4	0.5	0.97	0.96	0.92	0.95	0.98	0.98
Adams-Bohart model																		
K_{AB} (L/mg·min $\times 10^3$)	4	1.2	1.2	4	1.2	2	4	0.4	0.4	0.2	0.7	0.7	0.4	0.5	0.4	0.1	0.2	0.9
N_0 (mg/L)	1.1	0.17	0.55	0.4	0.18	0.24	0.45	0.49	0.85	0.66	0.44	1.11	0.53	0.49	1.36	0.94	0.62	1.16
R^2	0.94	0.88	0.93	0.95	0.93	0.92	0.98	0.93	0.94	0.94	0.88	0.98	0.99	0.96	0.92	0.92	0.96	0.99
Clark model																		
A	36.4	5.72	5.55	4.63	4.68	3.95	4.36	3.79	1.49	24.04	6.95	2.25	5.59	6.76	1.93	7.98	6.76	5.57
R	0.54	0.3	0.39	0.11	0.19	0.21	0.5	0.6	0.6	0.73	0.49	0.47	0.2	0.29	0.26	0.17	0.29	0.2
R^2	0.93	0.93	0.97	0.93	0.97	0.89	0.93	0.92	0.9	0.91	0.97	0.95	0.92	0.96	0.93	0.93	0.96	0.97

The Design Expert 13.0 software (evaluation version) was employed to estimate the coefficients of the proposed model, utilizing the matrix calculations provided by the software. The comparison between the estimated values obtained through the full factorial design model and the experimental results is illustrated in Figure 5.

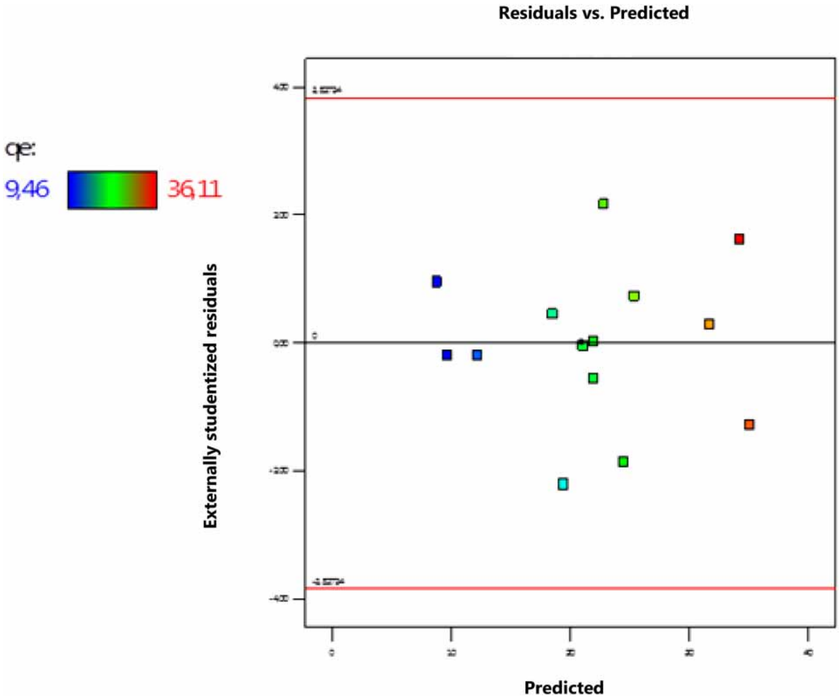

Figure 5 | Calculation of mean adsorption capacity through actual and residual values.

Table 2 shows that the R^2 value is 0.97, indicating that 97% of the adsorption capacity value is attributed to the three studied parameters (dye concentration, inlet flow, and bed depth). This suggests that the statistical model is effective in estimating the adsorption capacity value compared to the experimental measurement. The difference between the adjusted R^2 and R^2 is less than 0.0245, implying that the statistical model is consistent with the experimental outcomes. Additionally, the software utilized in this study enables for testing noise in the studied area, with an Adeq precision greater than 4, indicating acceptable precision. In this work, the Adeq precision of 33.015 indicates that the signal is appropriate.

Table 2 | Statistics parameter fit of ETL dye adsorption

Std. Dev.	1.54	R^2	0.9709
Mean	21.95	Adjusted R^2	0.9630
CV %	7.02	Predicted R^2	0.9385
		Adeq precision	33.0153

In Table 3 of the statistical analysis, the estimated coefficients of the model, standard error, and variance inflation factor (VIF) are presented. In this study, the VIF value is equal to 1, which indicates the orthogonality of the factors.

Table 3 | Estimation of the parameter effects on adsorption capacity

Factor	Coefficient estimate	Standard error	VIF
Intercept	21.95	0.3977	
A – bed depth	5.30	0.5446	1.0000
B – flow rate	−4.41	0.5446	1.0000
C – concentration	7.83	0.5446	1.0000

The linear model estimated to demonstrate the relationship between the coded parameters and the adsorption capacity is expressed as follows:

$$Y = 21.95 + 5.3A - 4.41B + 7.83C$$

When expressed as a function of the actual parameters, the estimated linear model is as follows:

$$q_e(\text{mg/g}) = 1.07837 + 4.239\text{BD} - 2.44794\text{FR} + 0.208867C$$

where BD is the bed depth (cm), FR is the feed flow rate (mL/min), and C is the initial concentration (mg/L).

The mathematical formulation derived from the full factorial design provides the opportunity to determine the significant order of the influence of operating dynamic parameters of the column. This ranking is based on the coefficients of the formula and is represented as follows:

$$\text{BD} > \text{FR} > C$$

Figure 6 presents both a 2D (a) and 3D (b) representation of the relationship between adsorption capacity and dynamic parameters.

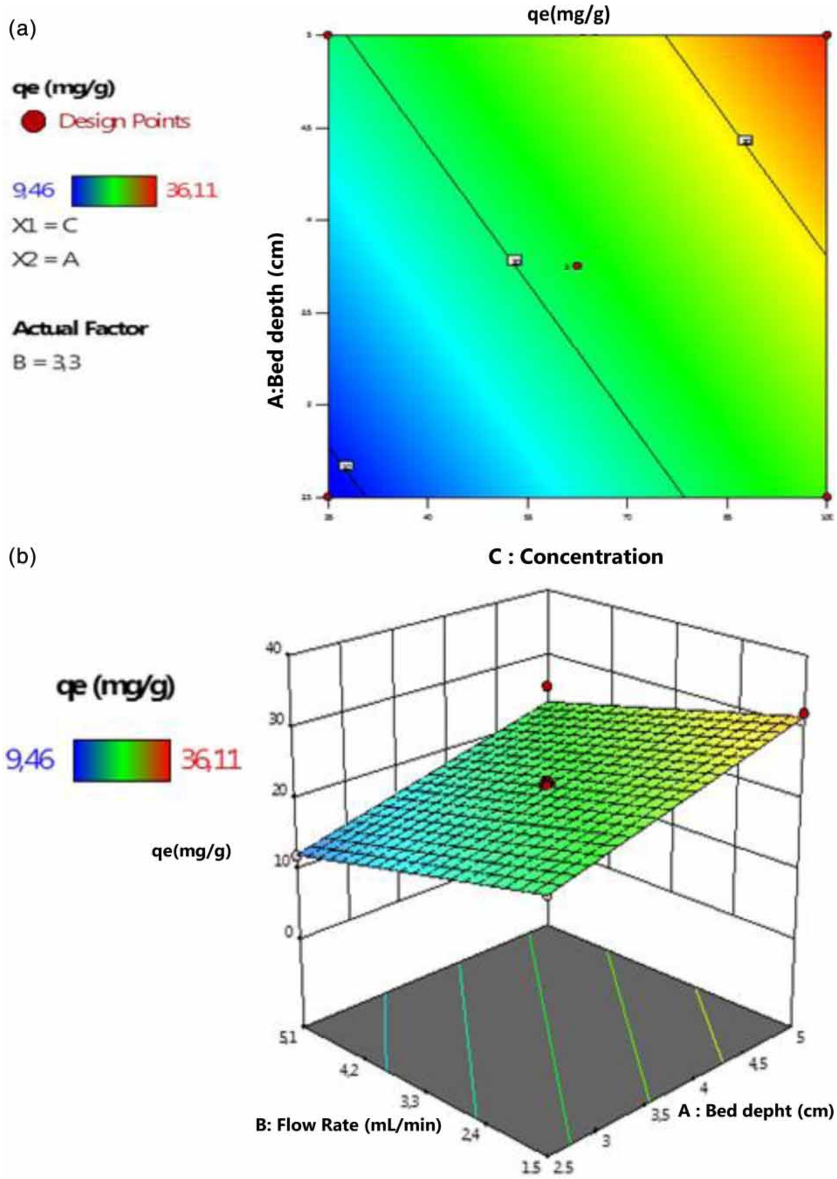

Figure 6 | (a) Contour plot of ETL dye adsorption and (b) 3D response surface of ETL dye adsorption at $C = 62.5$ mg·L^{-1}.

Figure 6 enables the deduction of additional values for the adsorption capacity from the studied area. Based on the statistical tests and diagrams, the polynomial model is considered a valid representation of the experimental design. This model allows for the prediction of responses for other values included in the studied area.

The color degradation in Figures 5 and 6 indicates that the adsorption capacity is positively influenced by the dye concentration and bed depth, whereas the inlet flow has a negative effect on dye removal. The same observations are recorded in the dynamic study.

CONCLUSION

The dynamic study confirms that brewery waste is effective in removing Bemacid red dye from aqueous solutions. Several dynamic models (BDST, Thomas, Adams-Bohart, and Clark) were used to analyze BTCs in the packed bed column. The BDST model describes the initial part of the curve, while the Thomas model fits well to the entire curve under the selected operational conditions. The results suggest that to increase the amount of dye removed, low flow rates, higher bed altitudes, and high dye concentrations should be used. The Thomas model has a high determination coefficient (R^2 ranging from 0.93 to 0.98) under these dynamic conditions. The full factorial design was used to model the adsorption capacity of brewery waste for the studied factors (bed altitude, dye concentration, and flow rate) using a first-degree polynomial model. This approach provides the degree of dependence between the response (adsorption capacity) and the factors, which was approximately 98% in our study.

FUNDING

The present research did not receive any financial support.

DATA AVAILABILITY STATEMENT

All relevant data are included in the paper or its Supplementary Information.

CONFLICT OF INTEREST

The authors declare there is no conflict.

REFERENCES

Al-Baidhany, J. H. & Al-Salihy, S. T. 2016 Removal of methylene blue dye from aqueous solution by using commercial granular activated carbon with different types of adsorbers. *Mesopotamia Environmental Journal* **2**, 1–11.

Almeida, E. J. R. & Corso, C. R. 2014 Comparative study of toxicity of azo dye Procion Red MX-5B following biosorption and biodegradation treatments with the fungi *Aspergillus niger* and *Aspergillus terreus*. *Chemosphere* **112**, 317–322.

Bennani, K. A., Mounir, B., Hachkar, M., Bakasse, M. & Yaacoubi, A. 2015 Adsorption of cationic dyes onto Moroccan clay: Application for industrial wastewater treatment. *Journal of Materials and Environmental Science* **6**, 2483–2500.

Bharathi, K. & Ramesh, S. 2013 Removal of dyes using agricultural waste as low-cost adsorbents: A review. *Applied Water Science* **3**, 773–790.

Bulgariu, L., Escudero, L. B., Bello, O. S., Iqbal, M., Nisar, J., Adegoke, K. A., Alakhras, F., Kornaros, M. & Anastopoulos, I. 2019 The utilization of leaf-based adsorbents for dyes removal: A review. *Journal of Molecular Liquids* **276**, 728–747.

Chowdhury, S., Yasin, M., Uddin, M. T. & Islam, M. A. 2016 Batch and continuous (fixed bed column) adsorption of methylene blue by rubber leaf powder. *International Journal of Integrated Sciences & Technology* **2**, 24–28.

Crini, G. & Badot, P. M. 2008 Application of chitosan, a natural aminopolysaccharide, for dye removal from aqueous solutions by adsorption processes using batch studies: A review of recent literature. *Progress in Polymer Science* **33**, 399–447.

García-Mateos, F. J., Ruiz-Rosas, R., Marqués, M. D., Cotoruelo, L. M., Rodríguez-Mirasol, J. & Cordero, T. 2015 Removal of paracetamol on biomass-derived activated carbon: Modeling the fixed bed breakthrough curves using batch adsorption experiments. *Chemical Engineering Journal* **279**, 18–30.

Gassan, H., Ben Driss Alami, S., Ochando-Pulido, J. M. & Víctor-Ortega, M. D. 2014 Iron removal from liquid effluents by olive stones on adsorption column: Breakthrough curves. *Ecological Engineering* **73**, 270–275.

Ghosh, A., Rechakrabarti, S., Biswas, K. & Dghosh, U. 2015 Column performance on fluoride removal by agglomerate Ce(IV)-Zr (IV) mixed oxide nanoparticles packed fixed –beds. *Journal of Environmental Chemical Engineering* **3**, 653–661.

Gupta, V. K. & Suhas, A. 2009 Review application of low-cost adsorbents for dye removal – A review. *Journal of Environmental Management* **90**, 2313–2342.

Hamdaoui, O. 2006 Dynamic sorption of methylene blue by cedar sawdust and crushed brick in fixed bed columns. *Journal of Hazardous Materials B* **138**, 293–303.

Hameed, B. H. 2009 Removal of cationic dye from aqueous solution using jackfruit peel as non-conventional low-cost adsorbent. *Journal of Hazardous Materials* **162**, 344–350.

Hutchins, R. A. 1973 New method simplifies design of activated carbon systems. *Chemical Engineering* **80**, 133–138.

Jain, A. K., Gupta, V. K., Bhatnagar, A. & Suhas, A. 2003 Utilization of industrial waste products as adsorbents for the removal of dyes. *Journal of Hazardous Materials* **101**(1), 31–42.

Kannan, K., Senthilkumar, K., Akilamudhan, P., Sangeetha, V. & Manikandan, B. 2012 Studies on effectiveness of low cost adsorbents in continuous column for textile effluents. *International Journal of Bioscience, Biochemistry and Bioinformatics* **6**, 398–402.

Kyzas, G. Z., Lazaridisand, N. K. & Mitropoulos, A. C. 2012 Optimization of batch conditions and application to fixed-bed columns for a sequential technique of total color removal using 'Greek coffee' residues as materials for real dyeing effluents. *Journal of Engineering Science and Technology Review* **5**(2), 66–75.

Manase, A. 2012 Fixed bed adsorption studies of rhodamine B dye using oil palm empty fruits bunch activated carbon. *Journal of Engineering Research and Studies* **3**, 03–06.

Ming-Shen, C. & Hsing-Ya, L. 2002 Equilibrium and kinetic modeling of adsorption of reactive dye on cross-linked chitosan beads. *Journal of Hazardous Materials B* **93**, 233–248.

Mobasherpour, I., Salahi, E. & Asjodi, A. 2014 Research on the batch and fixed-bed column performance of red mud adsorbents for lead removal. *Canadian Chemical Transactions* **2**, 83–96.

Muhamad, H., Doan, H. & Lohi, A. 2010 Batch and continuous fixed bed column biosorption of Cd^{2+} and Cu^{2+}. *Chemical Engineering Journal* **158**, 369–377.

Nihla Kamarudzamana, A., Chia Chayb, T., Amira, A. & Abdul Taliba, S. 2015 Biosorption of Mn(II) ions from aqueous solution by *Pleurotus* spent mushroom compost in a fixed-bed column. *Procedia – Social and Behavioral Sciences* **195**, 2709–2716.

Nishil, M., Grishkewich, N., Ambrose Waeijen, H., Berry R, M. & Chiu Tam, K. 2015 Continuous flow adsorption of methylene blue by cellulose nanocrystal – alginate hydrogel beads in fixed bed columns. *Carbohydrate Polymers* **09**, 1–23.

Nkem, Y., Abustana, I., Latiffa, M. F. P. M., Bello, O. S. & Ahmad, M. A. 2011 Fixed-bed column study for Cu (II) removal from aqueous solutions using rice husk based activated carbon. *International Journal of Engineering & Technology* **11**, 248–252.

Nouri, H. & Ouederni, A. 2013 Modeling of the dynamics adsorption of phenol from an aqueous solution on activated carbon produced from olive stones. *International Journal of Chemical Engineering and Applications* **4**, 4.

Ouazani, F., Iddou, A. & Aziz, A. 2017 Biosorption of Bemacid red dye by brewery waste using single and poly-parametric study. *Desalination and Water Treatment* **93**, 1–9.

Pei-Jen, L., Chih-Sheng, C. & Jia-Ming, C. 2014 Binary adsorption breakthrough curves in fixed bed: Experiment and prediction. *Journal of the Taiwan Institute of Chemical Engineers* **4**, 1608–1617.

Sekhula, M., Okonkwo, J. O., Zvinowanda, C. M., Agyei, N. N. & Chaudhary, A. J. 2012 Fixed bed column adsorption of Cu (II) onto maize tassel-PVA beads. *Chemical Engineering Process Technology* **3**, 1–5.

Shadeera, R. & Nagapadma, M. 2015 Modeling of fixed bed column studies for adsorption of azo dye on chitosan impregnated with a cationic surfactant. *International Journal of Scientific & Engineering Research* **6**, 538–545.

Sicupira, D. C., Tolentino Silva, T., Ladeira, A. C. Q. & Mansur, M. B. 2015 Adsorption of manganese from acid mine drainage effluents using bone char: Continuous fixed bed column and batch desorption studies. *Brazilian Journal of Chemical Engineering* **32**(02), 577–584.

Sivakumar, P. & Palanisamy, P. N. 2009 Packed bed column studies for the removal of Acid blue 92 and basic red 29 using non-conventional adsorbent. *Indian Journal of Chemical Technology* **16**, 301–307.

Wong, Y. C., Szeto, Y. S., Cheung, W. H. & McKay, G. 2004 Adsorption of acid dyes on chitosan – Equilibrium isotherm analyses. *Process Biochemistry* **39**, 693–702.

Yagub, M. T., Sen, T. K., Afroze, S. & Ang, H. M. 2014 Dye and its removal from aqueous solution by adsorption: A review. *Advances in Colloid and Interface Science* **209**, 172–184.

Yang, Q., Zhong, Y., Xiaoming, L., Xin, L., Luo, K., Xiuqiong, W., Hongbo, C., Yang, L. & Guangming, Z. 2015 Adsorption-coupled reduction of bromate by Fe(II)–Al(III) layered double hydroxide in fixed-bed column: Experimental and breakthrough curves analysis. *Journal of Industrial and Engineering Chemistry* **28**, 54–59.

Zümriye, A. 2005 Application of biosorption for the removal of organic pollutants: A review. *Process Biochemistry* **40**, 997–1026.

Zümriye, A. & Gönen, F. 2004 Biosorption of phenol by immobilized activated sludge in a continuous packed bed: Prediction of breakthrough curves. *Process Biochemistry* **39**, 599–613.

First received 10 July 2023; accepted in revised form 25 January 2024. Available online 27 February 2024